

Evaluation of a Solar Water Distiller Coupled With Solar Evacuated Tubes

Israa F Eldehn^{1*}, Mubarak M Mustafa², Mohamed F Atia², Mohamed A Salama¹, Yehia GM Galal¹, Mohamed A Hussien¹

1- Soil and Water Research Dept, Nuclear Research Center, Egyptian Atomic Energy Authority, Abou-Zaable, 13759, Egypt

2- Agricultural Engineering Dept, Fac of Agric, Ain Shams Univ, P.O. Box 68, Hadayek Shoubra 11241, Cairo, Egypt

*Corresponding author: IsraaFathy@agr.asu.edu.eg

<https://doi.org/10.21608/AJS.2022.134308.1478>

Received 17 April 2022; Accepted 4 July 2022

Keywords:

Active solar water distiller,
Ambient temperature,
Evacuated tubes collector,
Passive solar water distiller,
Solar radiation

Abstract: The scarcity of fresh water is a primary problem in remote regions. Thus, an economical and related water distillation solar still coupled with a solar collector was designed and studied experimentally. This study aims to investigate and evaluate the performance of an active single-slope solar still (ASSSS) coupled with a solar evacuated tube collector (ETC) as the water heater. The results showed that the average distillate productivity of ASSSS combined with U pipe solar (ETC) was 1.085 l/m² in December 2020, but 3.12 l/m² in August 2021. These quantities of the water distiller were higher than those of a passive solar distiller with a single slope (PSSSS). The average value of the water temperature increased using the ASSSS coupled with ETC in August 2021 at 79.1°C, whereas it was 71°C in August 2021 for PSSSS. These results indicate that the ASSSS is more effective than the PSSSS.

1 Introduction

Water purification can be proficient in various ways, including filtering and distillation. One of the most essential water purifying technologies is solar water distillation (Al-harashseh et al 2018). The radiation of the sun, ambient temperature, and basin water depth are the most important factors affecting on solar still productivity and efficiency (Kabeel and El-Agouz 2011). Depending on the energy source, solar water distillers can be classified as active or passive systems (Gugulothu et al 2015, Muftah et al 2014). Three elements determine the productivity of a solar still: environmental, operational, and design parameters. Solar

radiation and ambient temperature are examples of ambient conditions.

Sampathkumar et al (2012) tested the direct coupling between an active solar still with evacuated tubes and a passive solar still. The results showed that the water temperature increased with time. The active and passive solar stills produced the highest hourly yields of 1.12 and 0.62 kg per day, respectively. Singh et al (2013) investigated a solar distiller combined directly with an evacuated tube collector and found that the water temperature reached the highest value of the basin at 80°C and that the yield decreased further as the water depth increased. Issa et al (2017) established an active solar water distiller structure integrated with a solar collector using ETC to study the effect of evacuated solar tubes. The results showed that the

maximum daily output production values for the active solar distiller using ETC and the passive water distiller were 3.6 and 1.4 kg/m²/day, respectively.

According to Singh and Al-Helal (2018), an outside heat source, such as an evacuated tube collector with a heat exchanger, is employed to provide thermal energy to the basin in an active solar distiller. The fluid in the heat exchanger loop could be water or another appropriate liquid. This raises the thermal resistance and lowers the still's total performance (Bhargva et al 2020).

The objectives of this study are as follows:

- To evaluate the yield productivity, water temperature, and thermal efficiency of active or passive systems.
- To study economically analyze of both systems.

2 Materials and Methods

2.1 Site and system description

The system setup was installed at the Solar Energy Application Laboratory, Department of Agricultural Engineering at the Faculty of Agriculture, Ain Shams University, Egypt, located at 31° 09 N, 31° 30 E, and the altitude is 7 m above the sea level. In this study, two systems of solar stills were designed to compare the output water productivities and water temperatures of the solar distillation system. The experiment consisted of two systems:

- The first one was a passive solar distiller with a single slope (PSSSS), illustrated in **Fig 1-A**.
- The second one was an active solar distiller with a single slope (ASSSS) combined with a U pipe ETC illustrated in **Fig 1-B**.

Two simple solar distillers of identical dimensions were manufactured. Each of the solar stills was a square box basin with an area of 1 m² shown in **Fig 1-C, D**, **Table 1** show the specifications of the solar stills. The inner surface of the basin of the stills was painted black to maximize the amount of solar radiation absorption. Saline water entered the basin through a saline water tank, which was located above the basin. A water tube connected the water tank to the entrance of the stills. The experiment started from 8:00 am to 4:00 pm through the months October, December in 2020 and May, August in 2021. The water depth inside both basins was fixed at 1 cm. **Fig 2** shows the mechanical description for both systems.

2.2 Measuring parameters and devices

2.2.1 Measurements

In each solar still, ten thermocouples were used to measure different temperatures such as those of the water (T_w), inner glass cover (T_{gi}), outer glass cover (T_{go}), vapor (T_v), inner black wall (T_{bi}), and outer black wall (T_{bo}). **Fig 3** shows the location of the thermocouples inside the solar stills. In addition, inside humidity (H_i), ambient temperature (T_A), solar radiation (R_S), distillate output productivity (P_r), and total dissolved solids (TDS) were measured after and before distillation. The average values were obtained by calculating the mean value of four readings for the parameters under study every 15 min for 1 hour.

2.2.2 Calculations

• Internal heat transfer

The heat transfer process in a solar still can be broadly classified into internal and external heat transfer processes on the basis of the energy flow in and out of the enclosed space according to Patel et al (2019).

Heat transfer by radiation

$$q_{r,w-gi} = h_{r,w-gi} (T_w^4 - T_{gi}^4) \quad (1)$$

$$h_{r,w-gi} = \frac{\varepsilon_{eff} \sigma (T_w + 273)^2 + (T_{gi} + 273)^2}{(T_w + 273) + (T_{gi} + 273)} \quad (2)$$

where

q_{r,w-g} amount of heat transfer by radiation from the water to the glass cover (W/m²).

h_{r,w-g} heat transfer coefficient by radiation from the water to the glass cover (W/m².°C).

T_w water temperature (°C).

T_{gi} inner surface glass cover temperature (°C).

σ Stefan Boltzmann constant (5.67×10⁻⁸ W/m² K⁴).

ε_{eff} effective emission between the water to the glass cover

Heat transfer by convection

$$q_{c,w-gi} = h_{c,w-gi} (T_w - T_{gi}) \quad (3)$$

$$h_{c,w-gi} = 0.884 (\Delta T)^{\frac{1}{3}} \quad (4)$$

$$\Delta T = (T_w - T_{gi}) + \frac{(P_w - P_{gi}) * (T_w + 273)}{268.9 * 10^3 - P_w} \quad (5)$$

$$q_{e,w-gi} = h_{e,w-gi} (T_w - T_{gi}) \quad (6)$$

$$h_{e,w-gi} = 0.016273 * h_{c,w-gi} \left[\frac{P_w - P_{gi}}{T_w - T_{gi}} \right] \quad (7)$$

where

$q_{c,w-g}$ amount of heat transfer by convection from the water to the glass cover (W/m^2).

$h_{c,w-g}$ heat transfer coefficient by convection from the water to the glass cover ($W/m^2 \cdot ^\circ C$).

ΔT temperature difference between the water and the glass surface ($^\circ C$).

P_{gi} partial vapor pressure at inner surface glass temperature (N/m^2).

P_w partial vapor pressure at water temperature (N/m^2).

Heat transfer by evaporation

$$q_{t,w-gi} = q_{r,e-gi} + q_{c,w-gi} + q_{e,w-gi} \quad (8)$$

where

$q_{e,w-g}$ amount of evaporative heat transfer from the water to the glass cover (W/m^2).

$h_{e,w-g}$ evaporative heat transfer coefficient from the water to the glass cover ($W/m^2 \cdot ^\circ C$).

Total heat transfer from the water to the glass

Heat transfer by conduction between the inner and the outer glass cover

$$q_{cd,gi-go} = \frac{K_g}{L_g} (T_{gi} - T_{go}) \quad (9)$$

where

$q_{cd,gi-go}$ amount of heat transfer by conduction from the inner glass cover to the outer glass cover (W/m^2)

K_g thermal conductivity of glass ($W/m \cdot K$)

L_g thickness of glass

T_{gi} inner glass surface temperature ($^\circ C$)

T_{go} outer glass cover temperature ($^\circ C$)

• External heat transfer

Convection heat loss from the glass cover outer surface of the solar still to the atmosphere

$$q_{c,go-a} = h_{c,go-a} (T_{go} - T_a) \quad (10)$$

$$h_{c,go-a} = 2.8 + (3 * v) \quad (11)$$

where

$h_{c,g-a}$ convective heat transfer coefficient from the glass cover to ambient ($W/m^2 \cdot ^\circ C$)

$q_{c,g-a}$ amount of convective heat transfer from the glass cover to ambient (W/m^2)

T_{go} outer surface glass cover temperature ($^\circ C$)

T_a ambient temperature ($^\circ C$)

v wind velocity

Radiation heat loss from the glass cover outer surface of the solar still to the surroundings

$$q_{r,go-a} = h_{r,go-a} (T_{go} - T_a) \quad (12)$$

$$h_{r,go-a} = \epsilon_g \sigma \left[\frac{(T_{go} + 273)^4 - (T_{sky} + 273)^4}{T_{go} - T_a} \right] \quad (13)$$

where

T_{sky} temperature of sky ($^\circ C$) = $T_a - 6$

ϵ_g emissivity of the glass cover

Total top loss heat transfer

$$q_{t,go-a} = q_{r,go-a} + q_{c,go-a} \quad (14)$$

Rate of convective heat transfer between the solar still basin and the water mass

$$q_w = h_w (T_b - T_w) \quad (15)$$

where

h_w the convective heat transfer coefficient from the basin liner to the water

T_b basin temperature ($^\circ C$)

The rate of conduction heat transfer between the solar still basin to the atmosphere

$$q_b = h_b (T_b - T_a) \quad (16)$$

where

q_b amount of heat transfer from the basin liner to the ambient (W/m^2)

h_b overall heat transfer coefficient from the basin liner to the ambient through bottom insulation ($W/m^2 \cdot ^\circ C$)

- Thermal efficiency of the solar stills

The direct energy efficiency is given by the following relationship, and the overall thermal efficiency of the passive solar still is determined by the following expression:

$$\eta_{energy PSSSS} = \frac{m_{ew} * LH_w}{I_t * A_b * 3600} * 100\% \quad (17)$$

where

$I_{(t)}$ intensity of solar radiation over the inclined surface of the solar still (W/m^2)

m_{ew} hourly output from solar still ($kg/m^2 \cdot h$)

LH_w latent heat of water (J/kg)

A_b area of the solar still basin

The latent heat of evaporation is given in the following relation Gupta et al (2013).

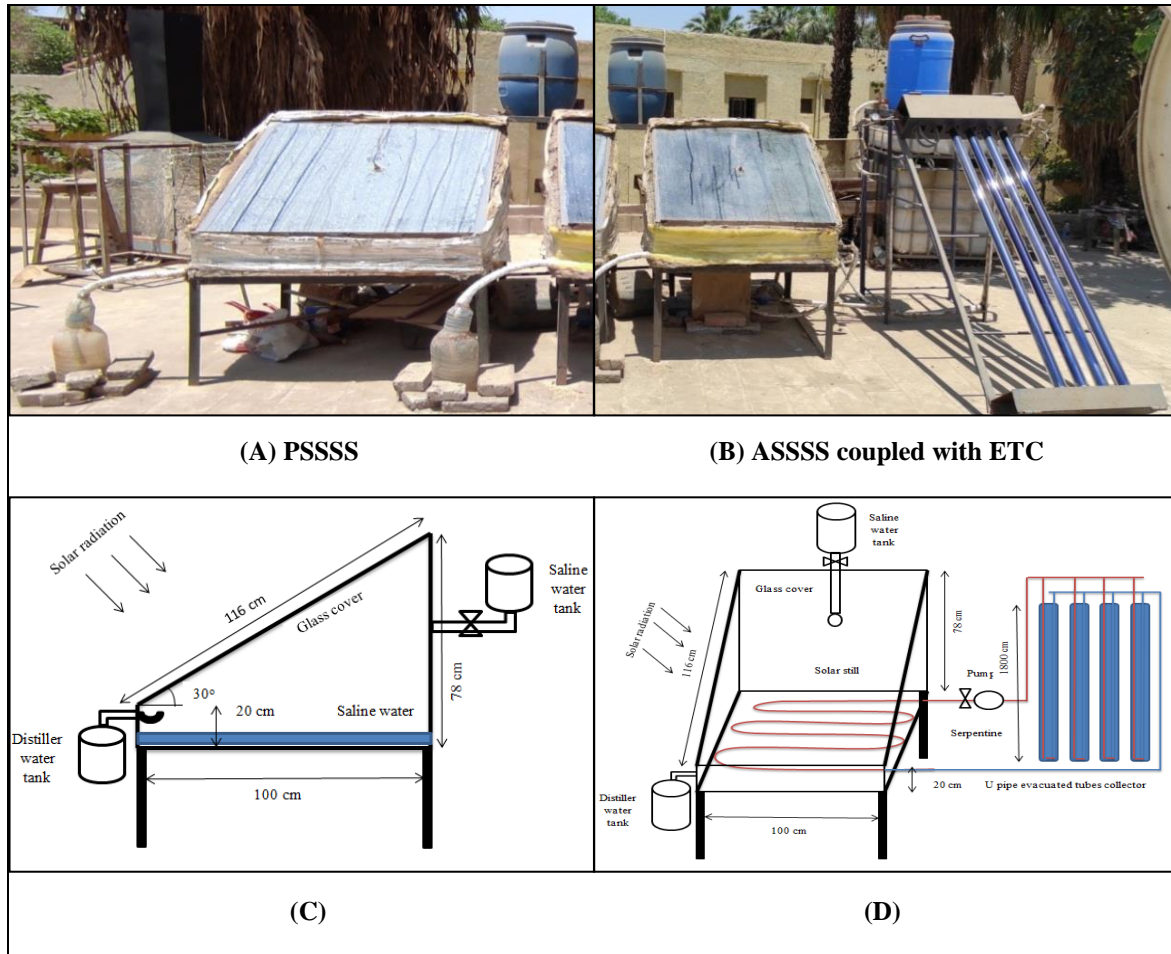


Fig 1. Schematic of (A) Passive solar still, (B) Active solar still

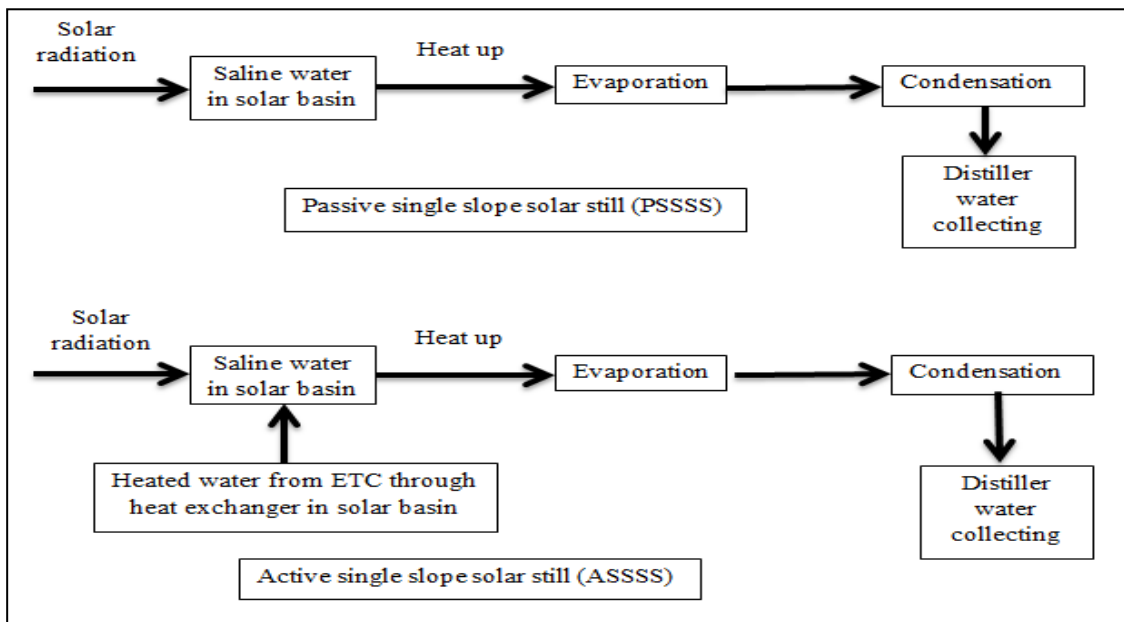


Fig 2. Mechanical description of the active and passive systems

Table 1. Characteristics of the solar still (SS)

Parameters		Value
Solar still	Area, m ²	1
	Front height (cm)	20
	Back height (cm)	78
	Thickness (mm)	0.8
	Material	Galvanized iron sheet
	Absorptivity of the basin (α_b)	0.90
	Transmissivity of the basin (τ_b)	–
	Emissivity of the basin (ϵ_b)	–
	Reflectance of the basin (ϵ_b)	0.1
	Specific heat of the basin (C_{pb}) (J/kg K)	490
	Galvanized iron absorptivity	0.77
	Galvanized iron density (kg/m ³)	7897
	Galvanized iron thermal conductivity (kW/m K)	72.7
	Water depth (cm)	1
	Transmissivity of water (τ_w)	0.95
	Reflectance of water (ϵ_w)	0.9
	Absorptivity of water (α_w)	0.05
	Glass wool density (kg/m ³)	50
	Glass wool thermal conductivity (W/m k)	0.042
	Glass wool specific heat (J/kg k)	670
Glass cover	Width (m)	1
	Length (cm)	116
	Thickness (mm)	6
	Absorptivity of the glass (α_g)	0.05
	Transmissivity of the glass (τ_g)	0.9
	Emissivity of the glass (ϵ_g)	0.9
	Reflectance of the glass (ϵ_g)	0.08
	Specific heat of the glass (C_{pg}) (J/kg K)	840
	Glass density (kg/m ³)	2700
	Glass thermal conductivity (W/m k)	0.78
Evacuated tubes	Outer tube glass diameter (cm)	5.8
	Inner tube glass diameter (cm)	4.7
	Length of the tube (cm)	1800
	Thermal conductivity of glass (W/m k)	0.74
	Absorptivity (α)	92%
	Emissivity (ϵ)	8%
	Tube number	4
Heat exchanger	Material	Copper
	Length (m)	7.5
	diameter	3/8"
	Copper thermal conductivity (W/m K)	385
	Working fluid	water
	Specific heat of the water (C_{pw}) (kJ/kg K)	4.18
	Water density (kg/m ³)	1000
Water thermal conductivity (W/m K)	0.591	

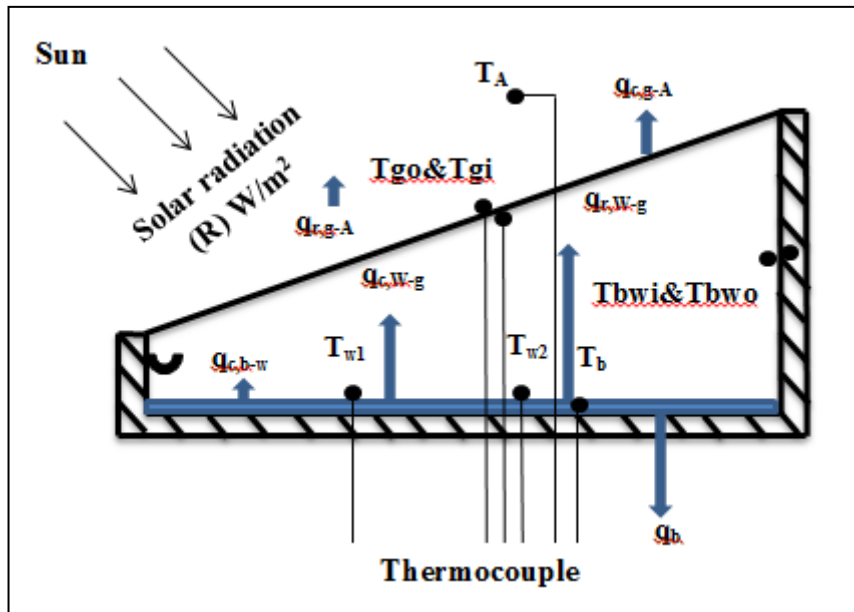


Fig 3. Location of thermocouples and heat transfer inside the solar stills

$$LH_w = 2.4935 * 10^6 [1 - 9.4779 * 10^{-4} * T_w + 1.3132 * 10^{-7} * T_w^2 - 4.7974 * 10^{-9} * T_w^3] \quad (18)$$

Also, the overall thermal efficiency of the active solar still is given as follows:

$$\eta_{energy\ ASSS} = \frac{m_{ew} * LH_w}{(I_t * A_s * 3600) + (I_t * A_{ETC} * 3600)} * 100\% \quad (19)$$

where
 A_{ETC} area of evacuated tubes collector (m^2)

2.2.3 Evaluation using instruments

The instruments used in this study are mentioned in **Table 2** including their measuring functions and accuracy.

2.2.4 Economic analysis

An economic study was done to estimate the annual price of the system per letter of output production (ac/l) in the current study using equations (4) to (10) in Kabeel and Abdelgaied (2017), as follows.

Let P be the initial amount invested in the solar still with the interest rate “i” per year and “n” be the useful life of the solar still in terms of years for which the given solar still can perform. Then, the capital recovery factor (CRF) can be calculated from **Eq. (20)**:

$$CRF = \frac{i * (1+i)^n}{(1+i)^n - 1} \quad (20)$$

The first annual cost (FAC) is calculated using **Eq. (21)**:

$$FAC = P * (CRF) \quad (21)$$

The sinking fund factor (SFF) is represented as follows:

$$SFF = \frac{i}{(1+i)^n - 1} \quad (22)$$

Therefore, the annual salvage value (ASV) is given as:

$$ASV = S * SFF \quad (23)$$

where
 S the salvage value of the solar still.

The total annual cost (TAC) of the solar still can be calculated by considering the annual operation and maintenance cost (AOMC) and the ASV as follows:

$$AOMC = 30\% FAC \quad (24)$$

$$TAC = FAC + AOMC - ASV \quad (25)$$

$$CPL = TAC/L = \frac{TAC}{M} \quad (26)$$

where
 M output productivity produced by the solar still, (l).
 CPL annual cost per l of distilled water productivity, EGP/l.

Table 2. Instruments used in this study

Instruments	Measuring Function	Accuracy	Variety
Solar power meter TM-207	Solar radiation	$\pm 10 \text{ W/m}^2$ or $\pm 5\%$	0~1999 W/m^2
Temperature Humidity meter	Steam temp. Inside humidity	$\pm 1^\circ\text{C}$ (- 30°C to + 40°C)	$R_t = -50^\circ\text{C}$ to + 70°C $R_m = 0\%$ to 99%
Digital thermometer	All temps.	$\pm(0.2\%+1^\circ\text{C})$	- 50°C to 199.9°C
Thermocouples K type	Probe	$\pm 1.5^\circ\text{C}$	- 50°C to 250°C
Waterproof EC/TDS Testers AD32	Total dissolved solids electric conductivity	$\pm 0.5^\circ\text{C}$ $\pm 2\% \text{ f.s. (TDS/EC)}$	0~20 ms/cm 0 to 10 ppt
Calibrated flask	Output productivity	$\pm 5 \text{ ml}$	0 to 1000 mL
Manometer	Water pressure inside serpentine	$\pm 0.5 \text{ bar}$	0 to 20 bar
Water flow meter Metrotec EGYPT	Water flow inside serpentine	0.0001 m^3	0 to $1.6 \text{ m}^3/\text{h}$

3 Results and Discussion

3.1 Variation of solar radiation and ambient temperature

This study aimed to raise the PSSSS distillate water productivity using solar evacuated tubes which were indirectly combined with the inner basin of the solar stills. The climatic conditions of the experimental site were solar radiation and ambient temperature. In this study, depending on the ambient temperature and solar radiation from October to December in 2020 and from May to August in 2021, the average monthly values of solar radiation were 919.2, 796.6, 782, 947.3, 953, 960 and 1031.3 W/m^2 , respectively as shown in **Fig 4-A**. Meanwhile, the average monthly values of the ambient temperature were 37.4°C , 31.3°C , 28.4°C , 39.8°C , 40°C , 40.1°C and 42.6°C as revealed in **Fig 4-B**. For the active solar distiller, the flow rate of water in the heat exchanger was remained fixed at 0.5 l/m. The performances of the active and passive solar distillers were verified at the same water depth of 1 cm and under the same climatic conditions.

3.2 Effects of solar radiation and ambient temperature on the solar distiller productivity

The solar distiller output depends on the ambient conditions of the site such as sun rays and ambient temperature. In **Fig 5**, the differences of in the average hourly values of the solar radiation and ambient temperature are shown with time through a random day in December 2020 and August 2021. In **Fig 5-A**, the ambient temperature

and solar radiation in December 2020 increased to the highest in the afternoon and decreased until 4:00 pm. The sun rays increased from 8:00 am to 12:00 pm and then reduced until 4:00 pm. the average highest and lowest values were 1039.5 and 413 W/m^2 in the afternoon and in the morning and evening, respectively. The ambient temperature had its average highest and lowest values at 33.2°C and 21.1°C , respectively.

In **Fig 5-B** the ambient temperature and solar radiation in August 2021 improved to the highest rate in the afternoon and reduced at 4:00 pm. The solar radiation gradually increased from 8:00 am to 12:00 pm and then reduced until 4:00 pm. It reached the average highest and lowest values were of 1189 and 260 W/m^2 in the afternoon and morning, respectively. The ambient temperature had its average highest and lowest values at 48.5°C and 29.4°C , respectively.

The ambient temperature tended to decrease from October to December 2020 and increased from May to August 2021. **Fig 6** shows the effects of the ambient temperature on the water temperature. The water temperature decreased from October to December 2020 and increased from May to August 2021. This showed that for the active solar distilled the average monthly temperatures of the water were 69.1°C in October 2020, 58.1°C in November 2020, 53.5°C in December 2020 and 69.4°C in May 2021, 72.7°C in June 2021, 72.8°C in July, 79.1°C in August 2021.

Fig 7 shows the variation in the average hourly values for the water temperature in both systems in December 2020 and August 2021, respectively. **Fig 7-A** shows that in the active solar distiller the average water temperature was 22.8°C at 8:00 am and increased up to 67.8°C at 12:00 pm, these then decreased

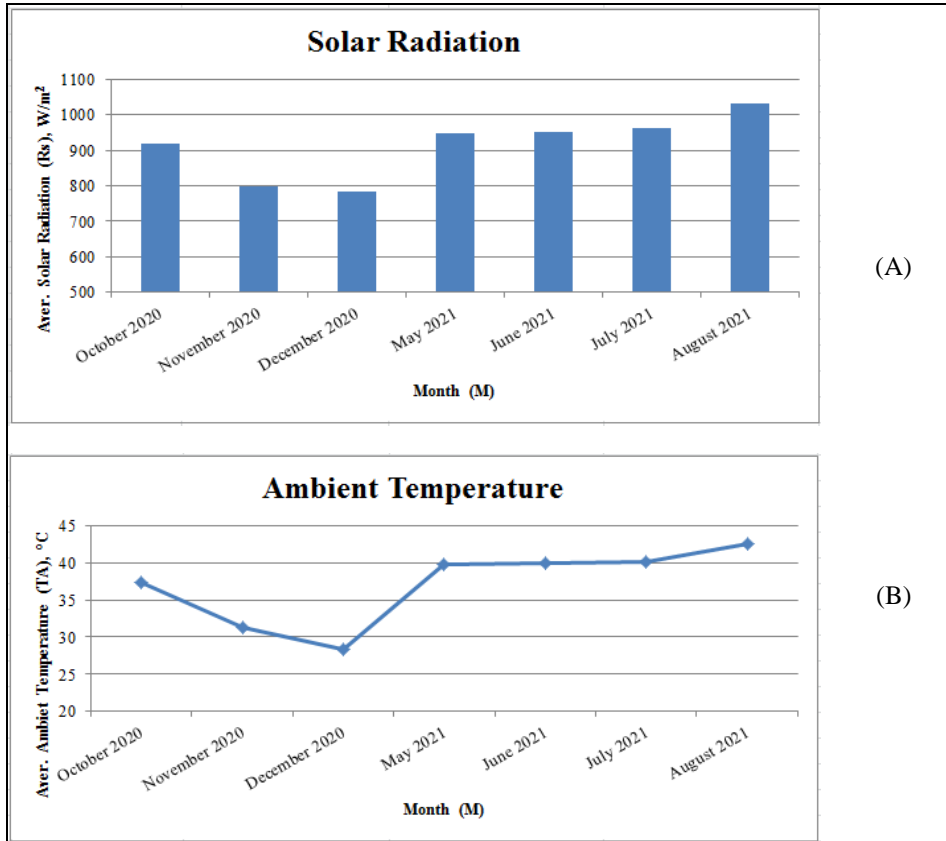


Fig 4. Average monthly values for the two systems (A) Solar radiation; (B) Ambient temperature

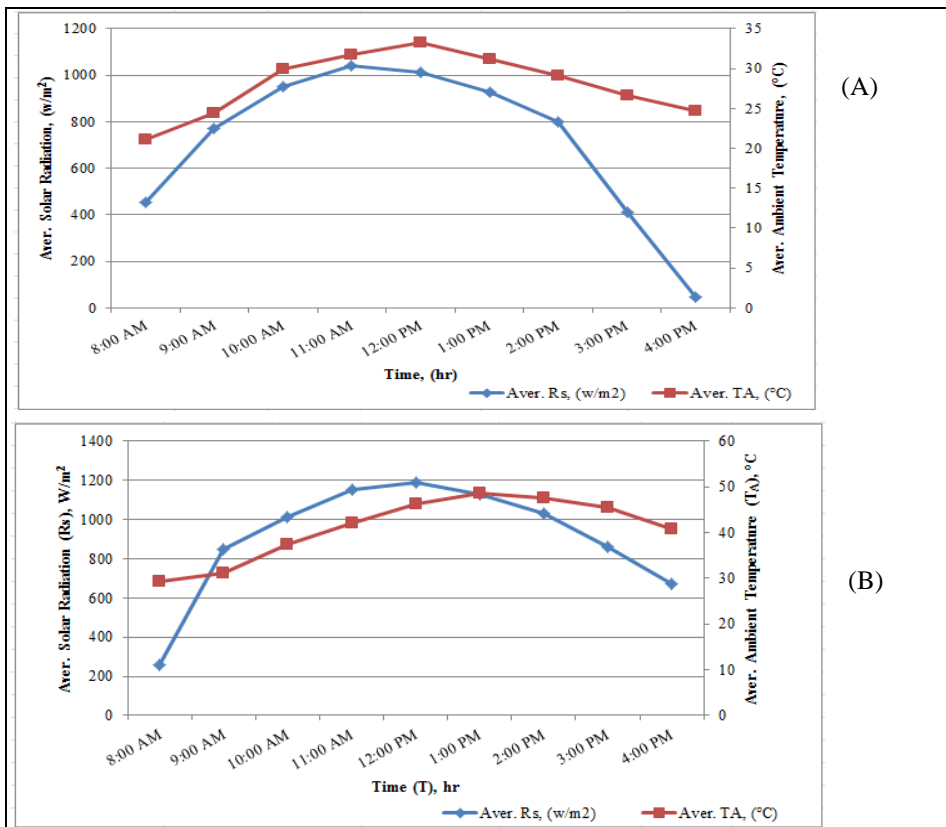


Fig 5. Average daily values of sun rays and ambient temperature for (A) December 2020, and (B) August 2021

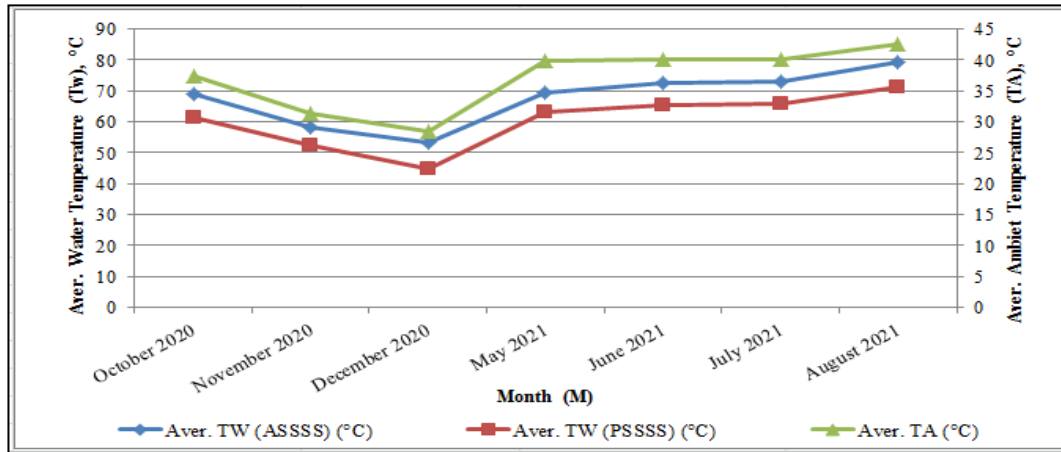


Fig 6. Average monthly measured temperature of water for the two systems

to 47.8°C at 4:00 pm. Meanwhile for the passive solar distiller the average water temperature was 18.6°C at 8:00 am and increased up to 57.8°C at 12:00 pm, then decreased to 41.1°C at 4:00 pm in December 2020. In addition to Fig 7-B showed that in the active solar distiller the average water temperature was 35.7°C at 8:00 am and increased up to 90.4°C at 12:00 pm, which then decreased to 70.5°C at 4:00 pm. Meanwhile in the passive solar still the average water temperature was 32.6°C at 8:00 am and increased up to 82.4°C at 12:00 pm, then decreased to 63.7°C at 4:00 pm in August 2021. The water temperature increased for solar active distiller from that of a passive solar distiller by 15% in December 2020. While in August 2021 the water temperature was increased for the active solar distiller from that of the passive solar distiller by 14%.

Fig 8-A, B shows the variation of all measured parameters used to evaluate the performance of these stills. The average ambient temperature, average solar radiation, the temperature of the average inside wall of the still, outside wall, steam, inside glass cover, outside glass cover and ETC in December 2020 were obtained. In addition to all measured parameters such as the average ambient temperature, average solar radiation, the temperature of the average inside wall of the still, outside wall, steam, inside glass cover, outside glass cover and ETC in August 2021. The shape of solar radiation and the variation of the temperature curve were very much similar to the expected theoretical curves for a clear day. In addition, the results showed that the measured temperatures such as those of water, steam, inner and outer wall of the

still, inner and outer glass covers increased in the morning to reach the highest value before it began to decline at 4:00 pm. The same performance was experimental for the shape of the sun rays during the study.

Fig 9 shows the variation of the average monthly productivity (amount of distilled water) in the months of October, November and December 2020 and May, June, July and August 2021 for the two still systems. It shows that the output distiller productivity reached its minimum value in December 2020 for ASSSS and PSSSS recording 1085 and 810 ml/m², respectively through 6 h. the output distiller productivity reached its maximum value in August 2021 for ASSSS and PSSSS recording 3120 and 2240 ml/day respectively. Meanwhile, the average increasing percentage reached through in October, November and December 2020 at 39%, 35% and 34%, respectively. It then reached 33%, 30%, 34% and 39% in May, June, July and August 2021, respectively.

The average hourly output productivities for the active and passive solar distillers during the day from 8:00 am to 4:00 pm in December 2020 and August 2021 are shown in Fig 10, Fig 10-A shows that in December 2020, the average hourly output productivity for the active solar distiller reached 1085 ml/m². It is higher than that of the passive solar distiller, which reached 810 ml/m². Fig 10-B showed that in August 2021, the average hourly output productivity for the active solar distiller reached 3120 ml/m². This is higher than that of the passive solar distiller, which reached 2240 ml/m². The main reason was that the rate of evaporation increased as the temperature of the water and the sun rays increased. The output water productivity was collected through a day in August 2021 for ASSSS and PSSSS. This showed an increase

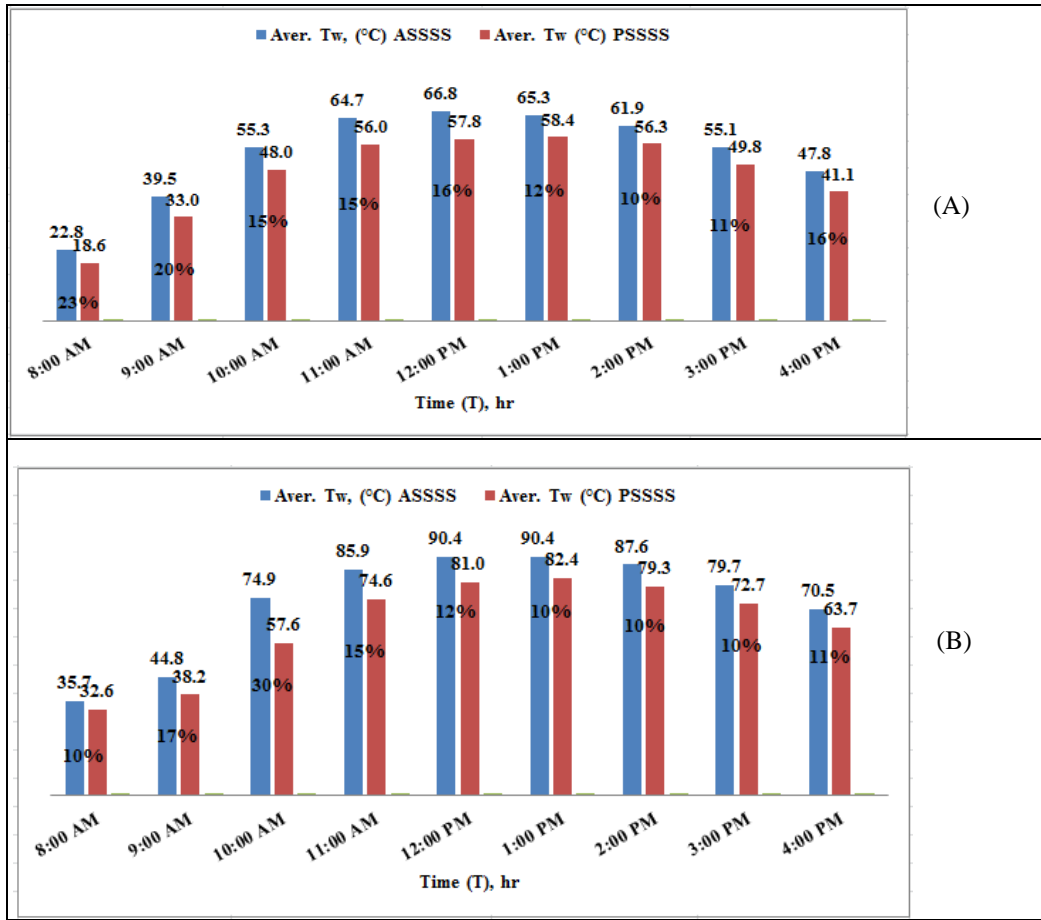


Fig 7. Average daily values of the water temperature and increasing percentage for both systems in (A) December 2020, and (B) August 2021

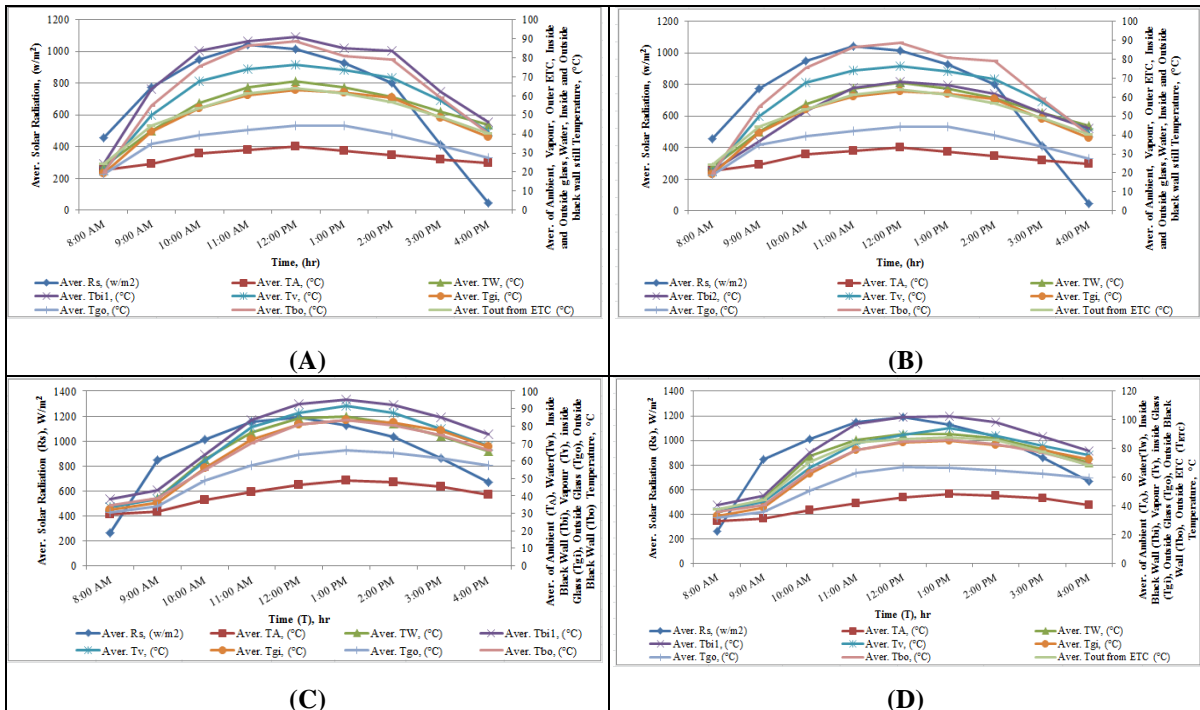


Fig 8. Variation of the solar radiation and ambient temperature on (A) PSSSS and (B) ASSSS in December 2020 and (C) PSSSS and (D) ASSSS in August 2021

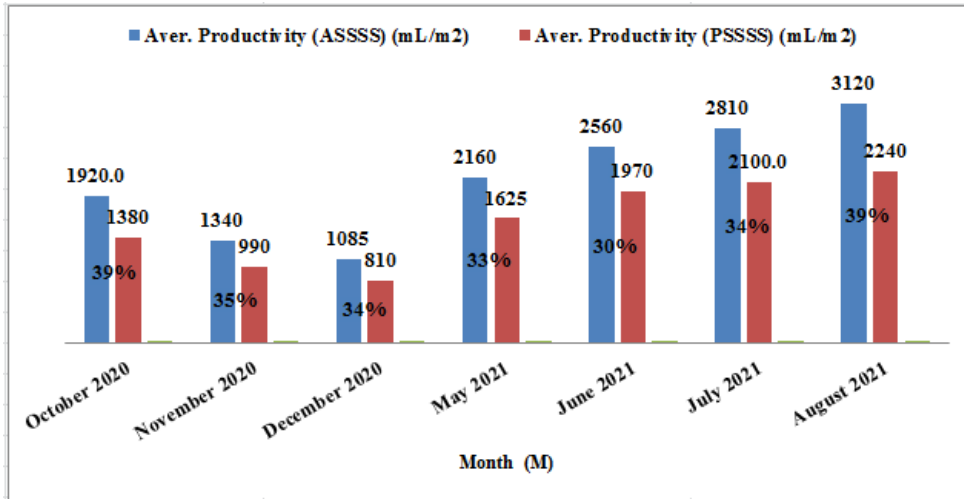


Fig 9. Average monthly values of the yield productivity and increasing percentage for the two systems

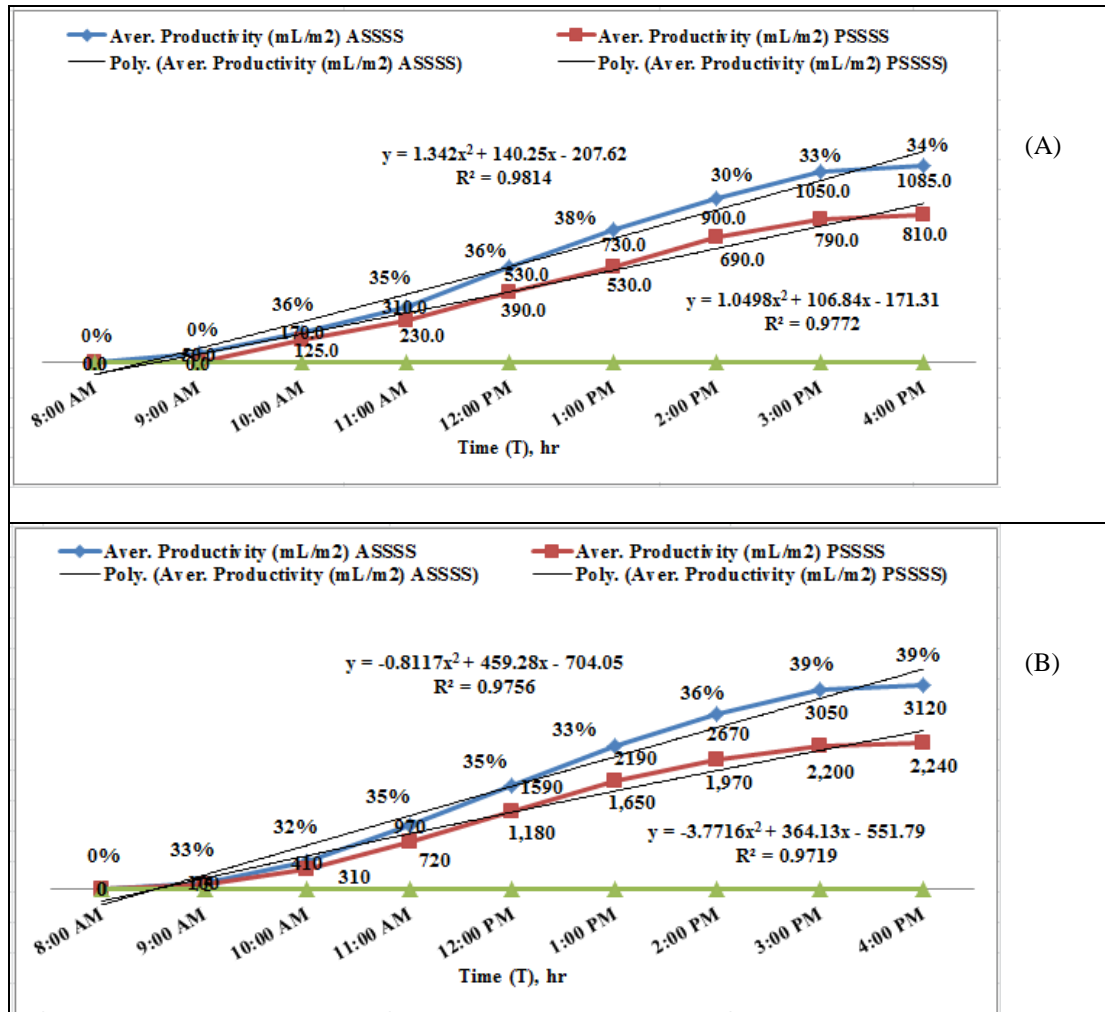


Fig 10. Average daily value of yield for both systems in (A) December 2020, (B) August 2021

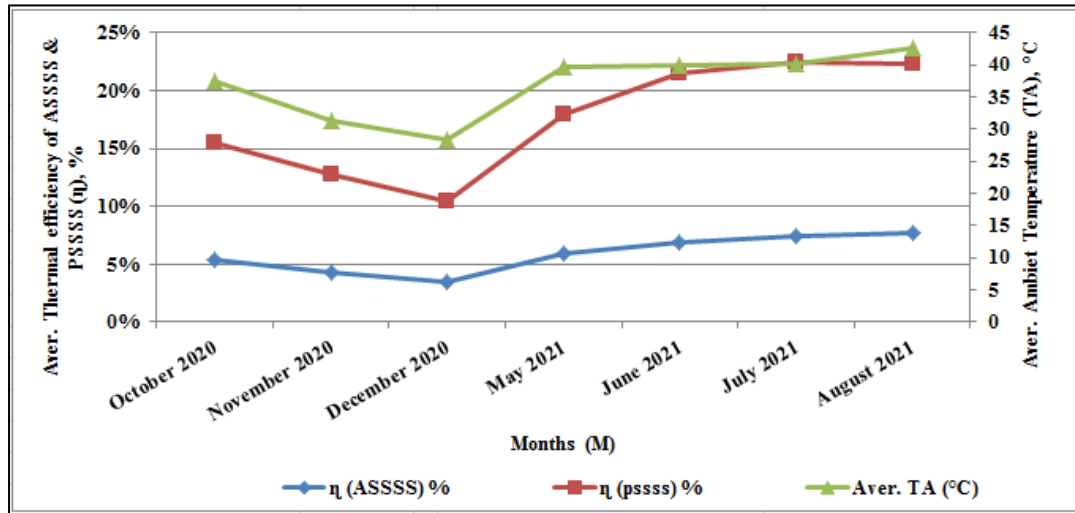


Fig 11. Variation of the thermal efficiency through the study months

in the amount of collected water at 8:00 am until it reached the highest yield around noon, matching the highest solar radiation and ambient temperature, and then decreased at 4:00 pm. The average increasing percentages were 34% in December 2020 and 39% in August 2021.

3.3 Effects of climatic conditions, water and inner glass temperatures on the thermal efficiency of solar stills

Fig 11 shows the thermal efficiency of PSSSS and ASSSS in different months (October, November and December in 2020) and (May, June, July and August in 2021). The thermal efficiency of the active solar still is lower than that of the passive solar still. Because of the higher operating temperature in ASSSS, the thermal energy loss increases. Hence, despite its higher yield, the efficiency of ASSSS decreases as compared with that of PSSSS.

3.4 Economic study

An economic study of the ASSSS and PSSSS systems is presented. The major advantage they effort is their zero solar energy cost. The total cost of the solar stills primarily involves the system setup, maintenance, and operation costs. The main determination of this study is to evaluate the economic possibility of the water distillation system for producing fresh water in certain regions. The lowest average productivities from 8:00 am to 4:00 pm can be valued at 2.83 and 1.98 l/m² for the active and passive solar distillers, respectively. The economic study was being done to estimate the annual price of the system per liter of output

production (ac/l) in the current study using equations (1) to (10) of Kabeel and Abdelgaied (2017). The approximate average productivity value for ASSSS in 1 year can be estimated as 1253 l/m²/year. For the PSSS, the corresponding value is estimated as 944 l/m²/year. For economic study calculations, the annual interest rate was assumed to be 12% for 10 years of useful solar still life, according to Kabeel and Abdelgaied (2017). The component cost and the annual cost calculations of the distillate output productivity of the ASSSS and PSSSS are 5405 and 2380, respectively. The annual cost /l of distilled water productivity EGP/L (ac/l) for ASSSS and PSSSS are 0.94 and 0.55 EGP/L, respectively.

4 Conclusions

The most important results could be summarized as follows:

- The U pipe ETC increased in output productivity throughout the study months.
- Similar trends were noticed with the variation of the water temperature throughout the study months under the U pipe ETC.
- The daily yield under all study months with the active solar distiller was increased by 35% which was more advanced than that of the passive solar distiller.
- The average water temperature through all study months with active solar distiller was increased by 12% which was more advanced than that of the passive solar distiller.
- From the investigation, the results showed that the modified solar distiller had a better performance than that of the passive solar distiller.

References

- Al harahsheh M, Abu Arabi M, Mousa H, et al (2018) Solar desalination using solar still enhanced by external solar collector and PCM. *Applied Thermal Engineering* 128, 1030-1040. <https://doi.org/10.1016/j.applthermaleng.2017.09.073>
- Bhargva M, Yadav A (2020) Experimental comparative study on a solar still combined with evacuated tubes and a heat exchanger at different water depths. *International Journal of Sustainable Engineering* 13, 218-229. <https://doi.org/10.1080/19397038.2019.1653396>
- Gugulothu R, Somanchi NS, Devi RSR, et al (2015) Experimental investigations on performance evaluation of a single basin solar still using different energy absorbing materials. *Aquatic Procedia* 4, 1483-1491. <https://doi.org/10.1016/j.aqpro.2015.02.192>
- Issa RJ, Chang B (2017) Performance study on evacuated tubular collector coupled solar still in west Texas climate. *International Journal of Green Energy* 14, 793-800. <https://doi.org/10.1080/15435075.2017.1328422>
- Kabeel AE, Abdelgaied M (2017) Observational study of modified solar still coupled with oil serpentine loop from cylindrical parabolic concentrator and phase changing material under basin. *Solar Energy* 144, 71-78. <https://doi.org/10.1016/j.solener.2017.01.007>
- Kabeel AE, El-Agouz SA (2011) Review of researches and developments on solar still. *Desalination* 276, 1-12. <https://doi.org/10.1016/j.desal.2011.03.042>
- Muftah AF, Alghoul MA, Fudholi A, et al (2014) Factors affecting basin type solar still productivity: A detailed review. *Renewable and Sustainable Energy Reviews* 32, 430-447. <https://doi.org/10.1016/j.rser.2013.12.052>
- Sampathkumar K, Senthilkumar P (2012) Utilization of solar water heater in a single basin solar still - an experimental study. *Desalination* 297, 8-19. <https://doi.org/10.1016/j.desal.2012.04.012>
- Singh DB, Al-Helal IM (2018) Energy metrics analysis of N identical evacuated tubular collectors integrated double slope solar still. *Desalination* 432, 10-22. <https://doi.org/10.1016/j.desal.2017.12.053>
- Singh RV, Kumar S, Hasan MM, et al (2013) Performance of a solar still integrated with evacuated tube collector in natural mode. *Desalination* 318, 25-33. <https://doi.org/10.1016/j.desal.2013.03.012>
- Patel J, Bhupendra KM, Subarna M (2019) Potable water by solar thermal distillation in solar salt works and performance enhancement by integrating with evacuated tubes. *Solar Energy* 188, 561-572. <https://doi.org/10.1016/j.solener.2019.06.026>